

UNIVERSITY OF MANITOBA

Mean Strain Field in a Conical Diffuser With
Fully Developed Flow at The Entry

by

M.S. Aulakh

A Thesis

Submitted to the Faculty of Graduate Studies
in Partial Fulfillment of the Requirements for the
Master of Science Degree

Winnipeg, Manitoba

1980

Mean Strain Field in a Conical Diffuser with
Fully Developed Flow at the Entry.

by

M. S. Aulakh.

A thesis submitted to the Faculty of Graduate Studies of
the University of Manitoba in partial fulfillment of the requirements
of the degree of

Master of Science

© 1980

Permission has been granted to the LIBRARY OF THE UNIVER-
SITY OF MANITOBA to lend or sell copies of this thesis, to
the NATIONAL LIBRARY OF CANADA to microfilm this
thesis and to lend or sell copies of the film, and UNIVERSITY
MICROFILMS to publish an abstract of this thesis.

The author reserves other publication rights, and neither the
thesis nor extensive extracts from it may be printed or other-
wise reproduced without the author's written permission.



ABSTRACT

An experimental study of the mean strain field in a conical diffuser having a total divergence angle of 8° and an area ratio of 4:1 with fully developed turbulent flow at entry is described. The data for mean static pressure and mean velocity (measured by a pitot tube) are presented for pipe Reynolds numbers of 56250 and 112500 based on pipe average velocity and the radius. The results of these two Reynolds numbers show, that the effect of Reynolds number on the flow is negligible, therefore most of the results are presented only for one Reynolds number of 112500, this was selected because higher Reynolds number flow is truly representative of turbulent flow. A high pressure gradient in the entry region of the diffuser produces a high mean radial velocity for this special kind of diffuser. In the first two-thirds of the diffuser, this radial velocity decreases in the downstream direction with increasing pressure. In the last third of the diffuser, the radial components of velocity tends to be constant along lines of constant radius (up to a radius of 1.4 times the inlet radius).

The mean axial flow velocity profiles (normalised with respect to the local centre line velocity and diffuser radius) show a straightening of the profiles over the first half of the diffuser and the development of reverse curvature further downstream. In the last four-fifths of the diffuser

there is a straight line starting at the wall, one fifth of the diffuser length from the entry, and running to the diffuser exit at a distance of two fifths of the exit radius from the axis.

The results of non-dimensional pressure gradient and friction velocity show that the relation between pressure gradient and friction velocity is linear.

ACKNOWLEDGEMENTS

The author wishes to express his deep sense of gratitude to Dr. R.S. Azad, Professor, Department of Mechanical Engineering (Thesis Supervisor) for his guidance, help and advice during the course of this work. Sincere thanks are due to Dr. J. Tinkler for his comments and careful review of the thesis.

Thanks are also due to the staff of the Department of Mechanical Engineering and fellow graduate students and Mr. K. Tart for assisting with the experimental set up. Thanks are also due to Mrs. P. Giardino for cheerfully typing the thesis, and Miss Kerry Hilton for her sincere help.

Last but not the least, I would like to express my indebtedness to my parents whose unselfish sacrifices made it all possible.

TABLE OF CONTENTS

	<u>Page</u>
ABSTRACT	i
ACKNOWLEDGEMENTS	iii
TABLE OF CONTENTS	iv
LIST OF TABLES	vii
LIST OF FIGURES	viii
NOMENCLATURE	xii
1.0 INTRODUCTION	1
1.1 Objectives	3
1.2 Developing Nature of Diffuser Flow and its Relationship with Wall Bounded Flow	4
1.3 Scope of the Present Study	5
2.0 LITERATURE SURVEY	6
3.0 WIND-TUNNEL EQUIPMENT	9
3.1 Basic Wind-Tunnel Equipment	9
3.2 Peripheral Wind-Tunnel Equipment	10
3.3 Wind-Tunnel Calibration	10
3.4 Wind-Tunnel Warm-up and Stability	13
3.5 Wind-Tunnel Vibration, Leaks and Resonance	14
4.0 MEASURING EQUIPMENT	16
4.1 Traversing Mechanism	16
4.2 Co-ordinate Table	16

	<u>Page</u>
4.3 Travel Micro-stage with Double Counter Micrometer Head	17
4.4 Vertical Slide with Probe Holding Tube Rod	17
4.5 Pitot and Static Pressure Probes	18
4.6 Circular Milling Attachment (Manual Type)	18
5.0 EXPERIMENTAL RESULTS AND DISCUSSION	19
5.1 Flow Specification	19
5.2 Mean Static Pressure	20
5.3 Axisymmetric Flow	24
5.4 Reliability of Data	25
5.5 Mean Axial Velocities in Axial and Radial Direction	26
5.5.1 Mean axial velocities in axial direction	26
5.5.2 Mean axial velocities in radial direction	27
5.6 Mean Radial Velocities in Radial and Axial Direction	30
5.6.1 Mean radial velocity in radial direction	30
5.6.2 Mean radial velocity in axial direction	31
5.7 Mean Axial Velocity Profiles in Radial Direction (Velocities are Normalized by Centreline Velocity)	32
5.8 Derivatives of Mean Axial Velocity in Radial and Axial Direction	32

	<u>Page</u>
5.8.1 Derivatives of mean axial velocity in radial direction . . .	32
5.8.2 Derivatives of mean axial velocity in axial direction . . .	34
5.9 Derivatives of Mean Radial Velocity in Radial and Axial Direction	35
5.9.1 Derivatives of mean radial velocity in radial direction . . .	35
5.9.2 Derivatives of mean radial velocity in axial direction . . .	36
5.10 Distribution of Non-Dimensional Pressure Gradient, Derivatives of Mean Axial Velocity at the Wall in Radial Direction, Friction Velocity and Shear Stress . . .	37
5.11 Ratio of Axial Derivatives of Mean Radial Velocity to the Radial Derivatives of Mean Axial Velocity . . .	39
5.12 Mean Strain Field in the Diffuser . . .	40
5.13 Relationship of The Strain Field to The Turbulent Flow Field	41
6.0 CONCLUDING REMARKS	43
7.0 RECOMMENDATIONS	45
REFERENCES	46
APPENDIX A.1 - Calculations of Mean Velocity	49
APPENDIX B - The Diffuser Mean Strain Data	50
TABLES	51
FIGURES	87

LIST OF TABLES

<u>Table</u>		<u>Page</u>
1	Mean flow parameters at the reference station	51
2	Axial stations are the distances from the exit of the diffuser in cm	52
3	($P_w - P_s$) static pressure data in mm of water	53
B-1 to B-27	The diffuser mean strain data measured in the laboratory, and calculated data . . .	60

LIST OF FIGURES

<u>FIGURE</u>		<u>Page</u>
1	Line diagram of flow circuit	87
2	Wind tunnel calibration	88
3	Fan speed calibration	89
4(a)	Photograph showing traversing mechanism, angle measuring circular attachment, travel micro-stage and vertical slide with probe holding tube rod	90
4(b)	Photograph showing pipe from contraction cone resting on trolleys	91
5(a)	Total pressure tube	92
5(b)	Static pressure tube	93
6(a)	Diffuser geometry	93
6(b)	Diffuser geometry showing representatives three regions I, II and III for total strain in axial direction and line of constant mean axial velocity, radial derivatives of mean axial velocity, maximum turbulent shear stress and maximum q^2 ($q^2 = u^2 + v^2 + w^2$)	94
7	Non-dimensional mean axial velocity normalized by pipe bulk average velocity at the reference station	95
8	Universal velocity profile at the reference station	96
9	Mean static pressure distribution	97
10	Triangular effectiveness plot for the pressure recovery coefficient	98
11	Mean static pressure gradient in the diffuser	99

<u>FIGURE</u>	<u>Page</u>
12	Variation of mean static pressure 100
	(a) Station 0, 1, 4, 7, 10 43 100
	(b) Station 46, 49, 52 76 101
	(c) Station 0, 43 and 76 102
13	Mean axial velocity profiles on both sides of the diffuser axis 103
	(a) Stations 0, 7, 13, 19, 25, 31 73 103
	(b) Stations 1, 4, 10, 16, 22, 28 76 104
14	Distribution of areas obtained from individual mean axial velocity profiles for stations 0, 1, 4, 7, 10, 13 76 105
15	Distribution of mean axial velocity in axial direction for different radial positions ($X_2/(R)_{ref.}$); $U_1/(U_b)_{ref.}$; $Re = 56250$ 106
16	Distribution of mean axial velocity in axial direction for different radial positions ($X_2/(R)_{ref.}$); $U_1/(U_b)_{ref.}$; $Re = 112500$ 107
17	Mean axial velocity profiles; $U_1/(U_b)_{ref.}$ in radial direction; $Re = 56250$ 108
	(a) Stations 0, 7, 13, 19 73 108
	(b) Stations 1, 4, 10, 16, 22 76 109
18	Mean axial velocity profiles; $U_1/(U_b)_{ref.}$ in radial direction; $Re = 112500$ 110
	(a) Stations 0, 7, 13, 19 73 110
	(b) Stations 1, 4, 10, 16, 22 76 111
19	Mean axial velocity profiles in radial direction from non-dimensional radial position; $X_2/(R)_{ref.} = 1.0$ up to the wall of the diffuser 112
	(a) Stations 0, 7, 13, 19, 25 67 112
	(b) Stations 1, 4, 10, 16, 22 70 113
20	Mean radial velocity profiles in radial direction; $U_2/(U_b)_{ref.}$; $Re = 112500$ 114
	(a) Stations 0 to 37 114
	(b) Stations 40 to 76 115

FIGURE

Page

21	Distribution of mean radial velocity in axial direction for different radial positions ($X_2/(R)_{ref.}$); $U_2/(U_b)_{ref.}$; Re = 112500	116
	(a) Radial positions 0.10 to 1.00	116
	(b) Radial positions 1.10 to 1.90	117
22	Mean axial velocity profiles normalized by centreline velocity in radial direction; $U_1/U_{1,m}$; Re = 112500	118
	(a) Stations 0, 7, 13, 19, 25 and 31	118
	(b) Stations 1, 4, 10, 16, 22 and 28	119
	(c) Stations 34,40,46,52,58,64,70 and 76	120
	(d) Stations 37,43,49,55,61,67 and 73	121
23	Mean axial velocity profiles experimental and computed values from the polynomial in radial direction; Re = 112500	122
24	Distribution of derivatives of mean axial velocity in radial direction; Re = 112500 $\partial (U_1/(U_b)_{ref.})/\partial (X_2/(R)_{ref.})$	123
	(a) Stations 0 to 37	123
	(b) Stations 40 to 76	124
25	Mean axial velocity profiles, experimental and computed values from the polynomial in axial direction; Re = 112500	125
26	Distribution of mean axial velocity derivatives in axial direction; Re = 112500	126
	(a) Radial positions 0,.2,.3,.4,.5 and .6	126
	(b) Radial positions .6,.7,.8,.9, 1.0, 1.1 1.9	127
27	Mean radial velocity profiles, experimental and computed values from the polynomial in radial direction; Re = 112500	128

FIGURE

Page

28	Distribution of derivatives of mean radial velocity in radial direction; Re = 112500	129
	(a) Stations 76 to 58	129
	(b) Stations 55 to 40	130
	(c) Stations 37 to 0	131
29	Mean radial velocity profiles, experimental and computed values from the polynomial in axial direction; Re = 112500	132
30	Distribution of derivatives of mean radial velocity in axial direction; Re = 112500.	133
	(a) Radial positions 0.0, 0.1, 0.3, 0.5, 0.7 and 0.9	133
	(b) Radial positions 0.2, 0.4, 0.6, 0.8 and 1.0	134
	(c) Radial positions 1.1, 1.2, 1.3, 1.4, 1.5, 1.6, 1.7, 1.8 and 1.9	135
31	Distribution of non-dimensional pressure gradient and shear stress along the wall of the diffuser; Re = 112500	136
32	Ratio of axial derivatives of mean radial velocity to the radial derivatives of mean axial velocity; Re = 112500	137
33	The distribution of total strain at stations 19 and 58 in radial direction and their ratios and their reciprocals; Re=112500	138
34	The distribution of total strain in axial direction for radial positions $(X_2/(R)_{ref.})$ 0.6 and 1.5	139

NOMENCLATURE

AR	Diffuser area ratio, A_{x_1}/A_{in}
A_{x_1}	Local cross-sectional area
A_{in}	Inlet plane cross-sectional area
\bar{C}_p	Pressure recovery coefficient $(P)_{x_1} - (P)_{in} / \frac{1}{2} \rho (U_1)_{in}^2$
D	Pipe diameter
H	Shape factor; $H = \frac{\delta^*}{\theta}$
P_{cone}	Contraction cone static pressure drop
P_0	Stagnation pressure
P_s	Static pressure
P_{sw}	Wall static pressure
P_{dy}	Dynamic pressure
R	Pipe radius
R_d	Local radius of the diffuser
R_e	Reynolds number, $((U)R/\nu)_{ref.}$
U_1	Mean axial velocity
U_2	Mean radial velocity
U_b	Pipe bulk average velocity
$U_{1,m}$	Pipe or diffuser centreline velocity
U_*	Friction velocity, $(\tau_w/\rho)^{1/2}$
U^+	U_1/U_*
X_1	Axial distance measure from the diffuser inlet
X_2	Radial distance measured from the axis of the diffuser

$U_1' X_1$ Non-dimensional derivatives of mean axial velocity
in axial direction,

$$\partial(U_1/(U_b)_{\text{ref.}})/\partial(X_1/(R)_{\text{ref.}})$$

$U_1' X_2$ Non-dimensional derivatives of mean axial velocity
in radial direction,

$$\partial(U_1/(U_b)_{\text{ref.}})/\partial(X_2/(R)_{\text{ref.}})$$

$U_2' X_1$ Non-dimensional derivatives of mean radial velocity
in axial direction,

$$\partial(U_2/(U_b)_{\text{ref.}})/\partial(X_1/R_{\text{ref.}})$$

$U_2' X_2$ Non-dimensional derivatives of mean radial velocity
in radial direction,

$$\partial(U_2/(U_b)_{\text{ref.}})/\partial(X_2/(R)_{\text{ref.}})$$

Y Radial distance from pipe or diffuser wall

Y^+ Non-dimensional radial distance from the wall,

$$Y^+ = YU_* / \nu$$


α Total vertical included angle of diffuser

θ Boundary layer momentum thickness

ρ Air density

τ Total shearing stress

- μ Dynamic viscosity
 ν Kinematic viscosity
 ξ_1 Non-dimensional axial distance, $\xi_1 = X_1 / \langle R \rangle_{\text{ref.}}$
 ξ_2 Non-dimensional radial distance, $\xi_2 = X_2 / \langle R \rangle_{\text{ref.}}$
 ξ_3 Non-dimensional radial distance, $\xi_3 = Y / R_d$
 ξ_4 Non-dimensional local radial distance, $\xi_4 = X_2 / R_d$
() Denotes cross-section average quantity

 Wall position

Subscripts

- in Diffuser inlet plane
Out Diffuser outlet plane
ref. Reference station
s Static tube pressure measurement
w Wall

1.0 INTRODUCTION

The simplest example of completely wall-bounded flow, and perhaps the most commonly occurring in practise, is the flow in a circular pipe. A great deal of experimental and analytical effort has been directed towards the fully developed region where the turbulent energy transfer processes are in dynamic equilibrium.

A diffuser or recuperator is a passage which gradually increases in sectional area downstream and its function is to reduce the velocity of flow while, at the same time, preserving the total pressure head as far as possible. Thus, a diffuser is a device for converting velocity head or dynamic head into pressure head. Usually a diffuser is of conical form but this is not necessary.

For a perfect fluid and for steady flow in the absence of body forces we have by Bernoulli's theorem

$$\frac{(U_1)_{in}^2}{2g} + \frac{(P_s)_{in}}{g\rho} = \frac{(U_1)_{out}^2}{2g} + \frac{(P_s)_{out}}{g\rho}$$

while continuity requires that $U_{1in} A_{in} = U_{1out} A_{out}$. Here quantities with suffice 1 refer to the entry to the diffuser while those with suffix 2 refer to the exit and it is assumed that the flow is uniform at these sections. Hence we obtain

$$(U_1)_{in} (A)_{in} = (U_1)_{out} (A)_{out}$$

This equation gives the pressure recovery in a perfect diffuser but in practice the ideal pressure recovery must be multiplied by a factor which is necessarily less than one. This factor depends on the nature of the surface but mainly on the nature of the flow at entry and on the angle of the cone. Let α be the total vertical angle of the cone. When α is very small the flow will adhere to the wall of the diffuser but the total resistance will be large because, with a given value of $(A)_{out}/(A)_{in}$, the diffuser will be long when α is small. The resistance will again be large when α is large because the flow will break away from the wall of the diffuser and energetic eddies will be formed, leading to much dissipation of mechanical energy. Evidently there is an intermediate value of α for which the pressure recovery is a maximum and it is generally accepted that this is in the neighbourhood of 8 degrees.

Experiments by Winternitz and Ramsay (1957) indicate that the non-dimensional pressure recovery coefficient is approximately a linear function of $(\theta\alpha/d)$ where θ is the momentum thickness of the boundary layer (see 6.4 Mechanics of Fluids, Duncan, Thom and Young, 1962) at entry to the diffuser and d is the diameter there. The pressure recovery coefficient is

$$C_{pr} = \frac{(P_s)_{out} - (P_s)_{in}}{\frac{1}{2} \rho U_1^2},$$

where U is the mean velocity at entry. In a series of tests on straight diffusers of 5° and 10° total angle and with various values of θ produced by the use of wire screens to thicken the boundary layer, it was found that C_{pr} fell from about 0.8 to about 0.65 when $(\theta\alpha/d)$ increased from 0.02 to 0.1 where α is measured in degrees. The walls of the diffusers were commercially smooth and the expansion ratio of A_{out}/A_{in} was 4.

For the present study an 8° included angle conical diffuser, with an area ratio of 4 to 1, and fully developed pipe flow at the entry was utilized. Sovran and Klomp (1967) have also shown that such a diffuser possesses optimum pressure recovery characteristics. D.J. Cockrell and E. Markland (1963) have shown that the diffuser with an area ratio of 4 to 1 is the most efficient diffuser.

1.1 Objectives

Diffuser research is an ongoing project at the University of Manitoba. The primary experimental objectives were to obtain data on mean velocities in radial and axial directions in a two coordinate system treating flow as two-dimensional. The same entry conditions were used by Arora (1978) but the diffuser used in this study has different material and dimensions although total included angle is the same. The Reynolds number effect was studied

and indicates that there is no effect of Reynolds number on the flow as shown by mean axial velocity profiles drawn in radial and axial direction for 56250 and 112500 Reynolds numbers.* The mean axial velocities are non-dimensionalized by pipe bulk average velocities and radius by radius of the pipe. From Figures (15), (16) and 17(a), 17(b) and 18(a), 18(b) it is clear that the velocities are nearly the same for both the Reynolds numbers within experimental error. The distribution of static pressure along the diffuser is shown in Fig. (9) for three Reynolds numbers and it is nearly the same for all. Therefore it shows that there is no effect of Reynolds number on the flow. Thusly, most of the data is presented at one Reynolds number.

1.2 The Developing Nature of Diffuser Flow and Its Relationship with Other Wall Bounded Flows

The flow in a conical diffuser is a developing axisymmetric flow with adverse pressure gradient. Near the inlet it maintains many properties of the entering flow which, in this case, is fully developed pipe flow. The fully developed flow at the entry was used because flow is in equilibrium in all length and time scale and has a finite value. The developing flow is very complex and there exists intermittent flow which makes it difficult

to study the effect on the diffuser. The fully developed flow at the entry was used and the effect of diffuser was studied.

1.3 Scope of the Present Study

The mean strain field is defined as how the fluid is being stretched or contracted in radial and axial directions. Very little work has been done with a positive pressure gradient. Yaglom and a few others are working presently in this field. Dr. Azad has done a lot of work in this field. Experimentally, it is good because at certain distances from the axis the mean quantities at certain diameters are nearly the same, and also the flow at the entry is fully developed.

The ideas can be obtained for turbulence because turbulence takes energy from mean field. A mathematical model can be formed if strain field is known.

Another objective of this study was to try to get results of mean axial velocity and parameters calculated from mean axial velocity within $\pm 5\%$ accuracy and to compare them with other researcher's results.

2.0 LITERATURE SURVEY

An early comprehensive study of diffuser flow was reported by Gibson (1910); on the basis of systematic experiments with water, he correlated pressure recovery coefficient with divergence angle for a fixed area ratio. Patterson (1938) surveyed all the available data and deduced general rules for diffuser design. Since then a vast number of experimental and theoretical studies (e.g., Nikuradse, 1929; Fraser, 1956; Sprenger, 1959; Kline, Abbott and Fox, 1959; Cocanower, Kline and Johnston, 1965; Sovran and Klomp, 1956; Ackeret, 1967; Cockrell and King, 1967) have been devoted to the subject.

The results of these investigations have led to the following points on the performance of diffusers: the pressure recovery coefficient $(\langle P \rangle_{\text{out}} - \langle P \rangle_{\text{in}}) / \frac{1}{2} \rho \langle U_1 \rangle^2$ in tends to

- (i) Increase as the thickness of the turbulent boundary layer at inlet decreases;
- (ii) decrease as the region of boundary layer separation increases within the diffuser;
- (iii) decrease for curved diffusers as the angle of deflection of the axis increases;
- (iv) become independent of Reynolds number as the Reynolds number increases to the range of most engineering applications;

(v) vary as the diffuser divergence angle is increased and the area ratio kept constant with a maximum occurring at about 8° .

Very little work has been done on strain field in an adverse pressure gradient having fully developed flow conditions at the entry. In the past years, work has been done with diffusers having developing boundary layer flow entry conditions. Fraser was probably the first to report mean flow data for diffuser. He used a diffuser which has a 10° included angle. He reported data on mean quantities in the flow by tilting the probe at a 2.5° angle to minimize errors due to changes in mean flow direction. An analytical solution of the turbulence problems, particularly under conditions of non-homogeneity, is not possible, and the study must proceed experimentally. The experimental approach however, also presents serious difficulties. The high level of turbulence in the region of interest renders it difficult to make an accurate determination of mean velocity and derivatives in axial and radial direction. The measurements, therefore, become reliable and meaningful only if the experiment is done very carefully, keeping check on changes in velocity due to change in other variables.

The present study was intended to prove Monin and Yaglom's theory, and Fraser's (1956) study of an incompressible turbulent boundary layer in a conical diffuser with a 10-degree

included angle. Fraser used boundary layer in his study, and for estimating the c_f , the flow was treated as plane. Fraser used a total pressure probe of round shape having internal diameter of .71 mm while in the present study the total pressure tube is flat in the front because it is pinched from both sides from a round tube of diameter 1.24 mm. The total pressure tube is always away from the wall by .62 mm. In the present case the thickness of the sub-layer appears to be less than 1 mm because measurements done by the total pressure probe at different stations along the diffuser length show that it is within the region where the measurements of mean velocity cannot be done with this Pitot tube.

3.0 WIND-TUNNEL EQUIPMENT AND PROCEDURES

3.1 Basic Wind Tunnel Equipment

The basic wind tunnel equipment which was used in this study has been described by Azad and Hummel (1976) and Okwuobi and Azad (1973). Briefly, the tunnel is of low speed, open circuit design with a rough surfaced tripping element installed to initiate the turbulent boundary layer growth. The line diagram of flow circuit is shown in Figure 1. The flow develops along a test section consisting of several pieces of 101.6 mm internal diameter steel pipe with an overall length of 7.32 meters before discharging through a diffuser into the laboratory. Thusly equipped the mean operating speeds of the tunnel can range from 15 m to 75 m/sec. in the pipe at reference station. In summarized form, the principal tunnel specifications are as follows:

Tunnel drive:

400 V, 52.5 amp rated 25 h.p. D.C. motor (mfgr. Compton and Parkinson) with a "Varimag" controlled power supply for speed adjustment (mfgr. Lancashire Dynamo Ltd.).

Blower equipment:

Spring mounted centrifugal type fan with fixed blade angle. Fan diameter 2 ft., blade width 1 ft. Inlet flared 2 ft. diameter with variable pitch guide vanes. (mfgr.

Chicago Blower Co.).

Flow Conditioner section:

3 feet diameter duct partitioned by 6 medium mesh screens in two groups and provided with a canvas coupling section to reduce the transmission of fan vibration. Overall length is 2.23 metres.

Contraction cone:

Plaster of Paris and fiberglass construction, equipped with 2 static pressure rings to measure pressure drop across the cone. Contraction cone ratio 89 to 1.

3.2 Peripheral Wind-Tunnel Equipment

- Trimount Inclined Manometer (specific gravity 0.827)
- Hero methanol manometer (specific gravity 0.834) with adjustable inclination angle
- Magnetic pick-up device with pulse shaping amplifier for monitoring fan rotation rate and tachometer for measuring r.p.m.
- Wall mounted, mechanically aspirated psychrometer
- Standard mercurial Fortin-type barometer.

3.3 Wind-Tunnel Calibration

On the basis of Bernoulli's equation for ideal incompressible flow, we expect that the mean velocity in the pipe is related to the static pressure drop across

the contraction cone according to $U_1 \propto \sqrt{\frac{P_{\text{cone}}}{\rho}}$, where the air density ρ is a function of the barometric pressure, tunnel air temperature and the moisture content of the air. The proportionality factor in the above relation was determined from measurements of the mean velocity, the contraction cone static pressure drop, and the air density for several tunnel operating points. The data were plotted in Figure 2. The constant of proportionality obtained from the data on this graph is 4.70 for mean velocity which is close to the one obtained by Reichert (1974).

The mean velocities for the figure were computed by numerical smoothing and integration of the velocity profiles measured for the different tunnel operating points. Although by continuity, the mean velocity is necessarily independent of longitudinal position, the data used for the mean velocity calibration was taken at the reference station which is at 85 cms from the exit plane of the diffuser. At that point the flow was assumed to be fully developed and a rough check on the mean velocity was permitted by comparison with the three-quarter radius velocity.

The mean velocity calibration curve is a function of the geometry, length and roughness element of the pipe, but it is independent of the equipment upstream of the contraction cone. For this reason tunnel calibration is

not subject to drift. A calibration based on the fan r.p.m. the power input, or some similar parameter rather than the cone pressure will vary since the fan efficiency depends upon warm-up time, temperature, motor speed stability and tunnel leaks in the flow straightener section. These considerations suggest that a separate calibration against the cone pressure should be performed each time the fan speed is to be used as an indicator of the tunnel air speed. The variation of motor speed with contraction cone pressure is plotted in Figure 3. The motor speed was determined by electronic counting voltage pulses caused by a toothed wheel on the motor near magnetic pick-up and by tachometer.

Because of its response, the Betz manometer is particularly suited for monitoring the cone pressure drop. The Betz was replaced by a Trimount inclined manometer so that the high accuracy, wide range scale, and easy reading features of the Betz could be used for the total pressure tube traverse measurements. The tunnel speed adjustment was made easier by permanently mounting the Trimount near the motor speed controller. The Trimount was calibrated against the Betz cone pressure readings and a linear function was fitted to the data to facilitate conversion of the Trimount readings to mm of water. Because average readings of the cone pressure were potentially more difficult to make because of the faster response of the Trimount this was

compensated for by using fairly long leads to the contraction cone pressure taps.

3.4 Tunnel Warm-up and Stability

After the tunnel is turned on, the flow structure establishes itself quite quickly, however, the tunnel does not attain stable equilibrium with laboratory return loop for some time due to the heating of the air which occurs at the blower. The principal heat sources appear to be the fan bearings, which can conduct heat to the fan itself through the drive shaft. A certain amount of heating may also be due to friction at the fan blades. The result is that after motor speed adjustment the tunnel air temperature will rise and at a slower rate the ambient temperature of the laboratory will also rise. There was a difference of temperatures between tunnel air and laboratory air of the order of one degree in the case of lower speed, and three degrees in the case of high speed. The corresponding decrease in air density can be expected to affect both the mass flow rate down the pipe and the fan speed. Changes in bearing friction with temperature can also cause the fan speed to vary. The net effect is that the observed cone pressure tends to increase very slowly at the lower speed with time and increase faster at a higher speed. This contradicts Reichert's statement that the cone pressure decreases at

a high setting.

The Trimount reading was checked every time before taking measurements. The Trimount was mounted near the measuring equipment and it was calibrated with the other Trimount which is near the regulator. Both the Trimounts were showing the same values for certain setting. This way it was made easier to check on any variation caused by change in speed, change in temperature and suddenly shutting and opening the door. The pressure inside the laboratory will decrease due to opening the door. The Trimount reading was observed to increase at the lower and higher tunnel speed settings. Tunnel warm-up time was found to be about two hours for higher speed but it could vary with changes in room temperature and pressure as shown by Reichert (1974). For low speeds, a shorter tunnel warm-up is sufficient. Even after considerable warm-up time random variations in the motor speed occur as indicated by cone pressure fluctuations observed with slow response Betz manometer. Van Der Spiegel (1960) has estimated this motor speed variation to be $\pm .43\%$. Even after thermal equilibrium was established, there were occasional rapid increases or decreases in the tunnel air temperature of the order of two or three degree Fahrenheit corresponding to the automatic start-up or shut-down of the laboratory ventilation system.

3.5 Wind Tunnel Vibration, Leaks and Resonance

The tunnel is remarkably free from vibrations due to several specific design features. The fan itself is mounted

on a spring frame and the fan section is isolated from the contraction cone by a canvas coupling. The flow straightener section is supported by canvas straps. The pipe sections before the entry of the diffuser, having a total length of 7.32 metres, are quite heavy and a heavy gauge track and trolley system supports the pipes at several points on foam cushions Figure 4(b). The design of the fan was changed two times to minimize vibrations.

The effect of removal of the roughness section on the overall tunnel behaviour at the lowest speeds was of particular interest. The tunnel cone pressure dropped and hence mean velocity was observed to oscillate regularly over a period of approximately 3 seconds and with an amplitude of 2 mm of water. The sound level was measured in the laboratory at two Reynolds numbers and the values of Mach numbers calculated show that flow is subsonic.

4.0 MEASURING EQUIPMENT

4.1 Traversing Mechanism

The traversing mechanism Figure 4(a) and 4(b) was designed and constructed for the present work. The components of the traversing mechanism are discussed briefly in the following sections.

4.2 Co-ordinate Table

A two-dimensional longitudinal cross-feed milling table (Type FB-102, M.S. Tool Suppliers Ltd.) was used with a travel micro-stage and double counter micrometer head for distance measurements. The milling table has the following specifications:

Clamping surface of table:	57.5 cm x 24.0 cm
Longitudinal feed:	37.5 cm
Cross feed:	15.6 cm
Length of bed plate:	25.9 cm
Width of bed plate:	25.0 cm
Total height:	11.4 cm
Weight approx. lbs:	124

The co-ordinate table was mounted on steel mounting to match with the test section. The longitudinal feed of the co-ordinate table is about 37 cm while the length of the diffuser is 76 cm. In addition the probe used to dip as it was moved in the axial direction because of slackness in the slide. Therefore, measurements of mean axial velocity were done by moving the probe coarsely on the co-ordinate table and finely by moving the co-ordinate table itself, making sure the probe remains in the horizontal plane by using a sensitive level on the co-ordinate table.